Neurochemical Research (2019) 44:1602–1612
https://doi.org/10.1007/s11064-019-02784-7

ORIGINAL PAPER

PKM2 Involved in Neuronal Apoptosis on Hypoxic-ischemic Encephalopathy in Neonatal Rats

Qiuxia Wu[1,2] · Wenliang Ge[1] · Yuehua Chen[1] · Xiaoli Kong[2] · Hua Xian[1]

Received: 1 September 2018 / Revised: 18 March 2019 / Accepted: 19 March 2019 / Published online: 25 March 2019

Abstract

Pyruvate Kinase isozymes M2 (PKM2) is a glycolytic enzyme involved in glycolysis that decarboxylates phosphoenolpyruvate to pyruvate and generates ATP. PKM2 also plays a significant role in tumor growth, in cell division, angiogenesis, apoptosis and metastasis. In this study, we have investigated the role of PKM2 in cortical neurons which suffered hypoxic-ischemic encephalopathy (HIE) in newborn rats. Immunohistochemistry and Western blot analysis revealed the protein expression of PKM2 peaking at 24 h after HIE. Double immunofluorescence labeling showed that PKM2 was mainly located in the neurons of the ipsilateral cerebral cortex, not in astrocytes or microglia. The increased level of active caspase-3 and the decreased level of phosphorylated AKT (p-AKT) were consistent with the PKM2 expression. TUNEL staining assay showed that PKM2 may participate in neuronal apoptosis in the rat ipsilateral cerebral cortex. Silencing of PKM2 in primary cultures of cortical neurons using a specific siRNA reduced the expression of active caspase-3 and upregulated p-AKT expression. Taken together, the results indicate that PKM2 may be involved in neuronal apoptosis after HIE by a mechanism dependent on the inactivation of p-AKT.

Keywords PKM2 · Neuronal apoptosis · Hypoxic-ischemic encephalopathy · P-AKT

Introduction

Neonatal hypoxic-ischemic encephalopathy (HIE) is one of the most common causes of severe neurological handicap in newborns, as well as being commonly associated with a high mortality rate, poor prognosis and complex pathogenesis. It is commonly caused by perinatal asphyxia [1, 2]. The percentage mortality of affected newborns in the postnatal period is around 15–20%, plus an additional 25% of affected newborns will go on to develop severe and permanent neuropsychological sequelae [3]. Only a small percentage of infants with serious morbidity recover with no handicap [4, 5]. Such injuries in preterm infants typically lead to gray matter damage in the cortex, hippocampus, basal ganglia, and/or thalamus [6, 7]. The pathophysiology of neonatal HIE involves multiple stages of which the secondary stage (6–48 h after HIE) of HIE results in sustained excitotoxicity, oxidative stress, and mitochondrial dysfunction [8–10]. Extensive biochemical and histochemical research have detected evidence for necrosis and apoptosis following ischemic injury [11–14].

The rate-limiting enzyme in the last step of the glycolysis process is pyruvate kinase (PK), which decarboxylates phosphoenolpyruvate to pyruvate and generates ATP. PK includes four isotypes, PKL, PKR, PKM1, and PKM2 [15, 16]. The expression of L and R isotypes is tissue specific and is regulated by different promoters. Both in liver, kidney, and intestine, the L isotype is expressed, and in red blood cells we can see the R isotype is expressed [17–20]. In most adult differentiated tissues such as brain and muscle, PKM1 is expressed, while the PKM2 can be found in embryonic cells, adult stem cells, and cancer cells [18, 19, 21–23]. PKM2 under normal conditions has a low rate of expression and is present in neural progenitors in the subventricular zone, hippocampus and cerebellum [24]. Studies have shown that PKM2 is associated with cell apoptosis under the influence of the oxidative stress with H_2O_2 or UV light [25]. Apoptosis is also thought to occur when mitochondrial dysfunction occurs in HIE [3, 26]. Meanwhile, PKM2 silencing-induced

✉ Hua Xian
xianhua@ntu.edu.cn

[1] Department of Pediatric Surgery, Affiliated Hospital of Nantong University, Nantong 226001, Jiangsu, China

[2] Medical College of Nantong University, Nantong 226001, Jiangsu, China

cell death in cancer cells is mediated by the AKT signaling pathway [27]. However, the expression and roles of PKM2 in cortical neuronal cells during HIE have not been reported.

In this study, a modified Rice–Vannucci model and oxygen glucose deprivation(OGD) model were established to mimic the pathology of HIE [28, 29]. In a rat HIE model, we confirmed that the expression and distribution of PKM2 in the cerebral cortex and revealed its correlation to neuronal apoptosis for the first time. Furthermore, we analyzed the protein level of caspase-3, active caspase-3, AKT and p-AKT in both in vivo and in vitro models, while transfecting PKM2–siRNA into primary cultures of cortical neurons to explore the possible relationship between PKM2 expression and neuronal apoptosis by means of AKT inhibitory activity. Therefore, these results imply that PKM2 plays a role in neuronal apoptosis after HIE.

Materials and Methods

Rat HIE Model

All animal experiments were conducted in accordance with National Institutes of Health's Guidelines for the Care and Use of Laboratory Animals. The newborn rat HIE model is a modified Rice-Vannucci model [28, 30, 31]. Postnatal Day 7 Sprague–Dawley rats purchased from Department of Animal Center of Nantong University were anesthetized with ether inhalation. The rats underwent a surgery where the left common carotid artery was ligated on both ends using 6−0 silk surgical sutures and cut in the middle. The rat pups were put in a hypoxic sealed chamber (N_2 balanced with 8% O_2) at 37 °C for 2.5 h after 1.5 h of recovery. The sham-operated rats were given anesthesia and exposed the left common carotid artery but not ligated. The rats were sacrificed at 0 h, 3 h, 6 h, 12 h, 24 h, 48 h after hypoxia for further experiments.

2, 3, 5-Triphenyltetrazolium Chloride Monohydrate (TTC) Staining

At 24 h post HIE, rats were anesthetized and brains were harvested. The brains were sectioned into four 2 mm slices and soaked in a 2% TTC (Sigma, USA) solution at 37 °C (in dark place) for 30 min. The brain slices were then stored in 4% formaldehyde solution for fixing overnight. The infarct areas of the prepared TTC stained slices were analyzed by Image-Pro plus software.

Western Blot

For Western blot analyses, ipsilateral hemispheres from sham-operated and injured rats were collected at 0 h, 3 h, 6 h, 12 h, 24 h and 48 h after the injury and were stored at − 80 °C for later analysis. The frozen cortex samples were minced with eye scissors on ice, then well-distributed in lysis buffer (25 mM Tris–HCl (pH 7.6), 150 mM NaCl, 1% NP-40, 1% sodium deoxycholate, 0.1% SDS, 100 μM phosphatase inhibitors (ab201112, Abcam), 100 μM a cocktail of protease inhibitors (78430, Thermo Fisher Scientific) and 1 mM PMSF) and clarified by centrifugation for 20 min in a microcentrifuge at 4 °C. BCA protein assay was used to detect its protein concentration, the collecting supernatant was separated to SDS–polyacrylamide gel electrophoresis. Following which, the separated proteins were electro-transferred to a polyvinylidine difluoride membrane (Millipore, USA) at 300 mA for 1.5 h. It was then blocked with 5% non-fat milk. The membrane was incubated with primary antibodies at 4 °C overnight against PKM2 (anti-rabbit, 1:1000; Cell Signaling Technology), active caspase-3 (anti-rabbit, 1:500; Abcam), p-AKT (anti-rabbit, 1:1000; Cell Signaling Technology), AKT (anti-rabbit, 1:1000; Cell Signaling Technology) and GAPDH (anti-rabbit, 1:1000; Santa Cruz). After incubating with an anti-rabbit horseradish peroxidase conjugated secondary antibody (1:5000–10,000; Cell Signaling Technology), the protein was washed with TBS-T three times for 5 min. The protein bands were visualized via an enhanced chemiluminescence system (ECL, Pierce Company, USA).

Preparation of Frozen Section

The sham-operated groups and HI groups rats were euthanized at 24 h, following which all rats were perfused with heparinized saline at the above time points and fixed with 4% paraformaldehyde. Next, each brain was excised and immersion-fixed in 4% paraformaldehyde at 4 °C for 24 h. The brain was then dehydrated through graded sucrose (10%, 15%, and 30%) at 4 °C for 24 h at each grade. Frozen brain coronal sections cut at a thickness of 8 μm and then stored at − 20 °C for later use.

Immunohistochemical Staining

For immunohistochemistry staining, all sections were placed in the oven for 2 h at 37 °C and then blocked in 10% donkey serum for 2 h at room temperature. Next, all sections were incubated with primary antibodies against PKM2 (anti-mouse, 1:1000; Santa Cruz) at 4 °C overnight, followed by biotinylated secondary antibody (1:2000, Vector Laboratories, USA) at 37 °C for 30 min. All sections were reacted with the DAB (Vector Laboratories, USA) and finally visualized with Leica DM5000 microscope (Leica, Germany). Cells that were strong or moderate brown staining were considered positive, while weak or non-stained cells were considered negative.

Double Immunofluorescent Staining

Initially, each section was rewarmed at 37 °C for 2 h and then washed with PBS for 5 min. Subsequently, all sections were blocked with the buffer (10% donkey serum) and 1% Triton X-100 for 2 h, an incubation with primary antibodies against PKM2 (anti-mouse, 1:1000; Santa Cruz), NeuN (anti-rabbit, 1:100; Abcam), GFAP (anti-rabbit, 1:300; Abcam), Iba-1 (anti-rabbit, 1:100; Abcam), and active caspase-3 (anti-rabbit, 1:1000; Abcam) at 4 °C overnight. After 15 min PBS washing, all sections were incubated with the secondary antibodies (CY3-and FITC-Donkey, 1:300; Jackson Laboratory) in the dark for 2 h at 37 °C. After washing for three times, then the sections were assayed by Leica fluorescence microscope (Leica, Germany).

TUNEL Staining

We performed the TUNEL staining by utilizing an apoptosis detection kit (ApopTag Fluorescein in Situ Kit; Millipore, USA) according to the operation manual. The Sections were prepared as mentioned above and blocked with 1% Triton X-100 for 2 min. The sections were first rinsed with PBS and incubated with 50 µl TUNEL reaction mixture and labeling solution at 37 °C for 60 min, respectively. After washing three times with PBS for 15 min each, the staining results were analyzed using a Leica fluorescence microscope (Leica, Germany).

Rat Primary Cultures of Cortical Neurons Culture

Primary cultures of cortical neurons were derived from the cerebral cortex of embryonic day 15 pregnant Sprague Dawley rat. Under aseptic conditions, the dissected cerebral cortex was digested in 0.25% trypsin and plated on poly-L-lysine-coated (0.05 mg/ml in deionized water, Sigma, USA) 6-well plates (density of 1×10^6 cells/ml) and 24-well plates (density of 1×10^5 cells/ml). After culturing in a humidified incubator of 5% CO_2 at 37 °C for 4 h, the glucose-free Dulbecco's Modified Eagle's Medium (DMEM, Gibco, USA) was changed to being supplemented with 2% B27 (Gibco, USA) and serum-free Neurobasal medium (Gibco, USA), and the medium which was changed every 2 days.

OGD Treatment and Transfection

Primary cerebral cortex neurons were prepared as we mentioned previously. In brief, after replacing cell cultures with DMEM without glucose, the cultures were transferred to a hypoxia modular incubator chamber (Billups-Rothenberg, USA) filled with a gas mixture of 95% N_2 and 5% CO_2 at 37 °C. After 4 h of OGD treatment, the neurons were cultured again in Neurobasal medium supplemented with 2% B27 and returned to the 37 °C incubator of 5% CO_2 for 24 h before further experiment.

The neurons in the sham groups were grown in the medium (Neurobasal medium supplemented with 2% B27) in a humidified atmosphere (at 37 °C, 5% CO_2). For transfection, the siRNAs for PKM2 were purchased from Ribobio (Guangzhou, China). The PKM2–siRNA and control siRNA were transfected to neurons using lipofectamine plus reagent in OptiMEM according to the operational instructions. The PKM2 siRNA sequences were as follows: si-PKM2#1, TCCACCGCCTGCTGTTTGA; si-PKM2#2, GGCCTCTTATAAATGTTTA; si-PKM2#3, GCAGCT TTGATAGTTCTGA. After 48 h for transfection, cells were treated by OGD for 4 h and reoxygenation for 24 h.

Determination of viable cell number. Cells were inoculated at 2.5×10^4 cells/0.1 ml in a 96-microwell plate (Becton Dickinson Labware, Franklin Lakes, NJ, USA). Based on the OGD treatment and transfection section, after 48 h for transfection, cells were treated by OGD for 4 h and reoxygenation for 24 h. Control cells were treated with the same concentration of DMSO present in each diluent solution. Cells were incubated for 48 h and the relative viable cell number was then determined by the MTT method. In brief, the treated cells were incubated for another 3 h in fresh culture medium containing 0.2 mg/ml MTT. Cells were then lysed with 0.1 ml of DMSO and the absorbance at 540 nm of the cell lysate was determined using a microplate reader (Biochromatic Labsystem, Helsinki, Finland). The CC50 was determined from the dose–response curve and the mean CC50 for each cell type was calculated from three independent experiments.

Immunocytochemistry Staining

After OGD and reoxygenation, the transfected primary cultures of rat cortical neurons were cultured on coverslips for 24 h in 24-well plates. After 24 h culturing, the removed cell cultures were washed with PBS for 5 min and subsequently fixed in 4% paraformaldehyde for 30 min. After fixing, the cells were washed with PBS for three more times. The cells were then blocked with a buffer (10% donkey serum) for 2 h. The prepared coverslips were incubated with antibodies against PKM2 (anti-mouse, 1:1000; Santa Cruz) and active caspase-3 (anti-rabbit, 1:1000; Abcam) at 4 °C overnight. The coverslips were then incubated with the CY3 and FITC-donkey secondary antibodies (1:300; Jackson Laboratory) in dark at 37 °C for 2 h after washing cells with PBS. The images were captured by a Leica fluorescence microscope (Leica, Germany).

Statistical Analysis

We used GraphPad Prism 6.0 Software to analyze all data in our study. All values were expressed as mean ± standard error of mean (SEM). The statistical dissimilarities between the HIE group and the sham group were performed by one-way analysis of variance (ANOVA) followed by Student's t test. The statistically significant value was considered at $P < 0.05$.

Results

The TTC Staining Analysis and Infarct Areas After Modeling HIE

TTC staining is a relatively simple and rapid experimental method performed on fresh brain sections after modeling HIE, and preparations stained in < 60 min can be used for analysis. After a 3 h period of hypoxia and reoxygenation 24 h, TTC staining for serial slices of the neonatal rat brain which was from the same given animal were performed in the HIE group and the sham-operated group. As expected, the occurrence of HIE resulted in an infarct (Fig. 1), suggesting the HIE model established in this study was successful.

The Expression of PKM2 Protein Level Increased After HIE

In order to investigate PKM2 protein level from 0 to 48 h in the ipsilateral cerebral cortex after HIE, we performed the western blot analysis. PKM2 expression was comparatively low in the cerebral cortex of the sham-operated group. Compared to sham-operated rats, an increased expression of PKM2 was detected immediately after HIE and reached the maximum at 24 h. At 48 h post-HIE PKM2 expression was lower than at 24 h, it remained elevated in comparison to 0 h, 3 h, 6 h and 12 h after the injury (Fig. 2a, b).

The Distribution of PKM2 in the Ipsilateral Cerebral Cortex After HIE

To further corroborate the expression and distribution of PKM2 protein in the ipsilateral cerebral cortex after HIE, we applied immunohistochemistry to detect PKM2 protein at 24 h after HIE. In comparison with sham-operated group, PKM2 immunostaining signal was obviously enhanced in ipsilateral cerebral cortex at 24 h following HIE, which was in keeping with the western blot results (Fig. 3a–d). It can be seen from the data in Fig. 3e that PKM2-positive cells in brain cortex after HIE were increased remarkably. From these data, it was apparent that PKM2 was up-regulated in neurons after modeling HIE.

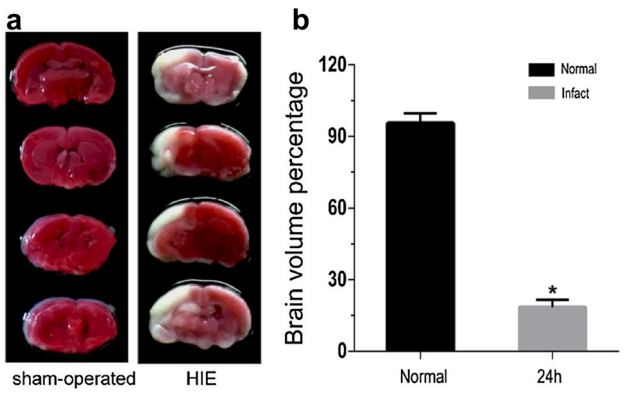

Fig. 1 Infarct volume in the newborn rat brain sections after modeling HIE by TTC staining. **a** The representative pictures of 24 h time point HIE group and sham-operated group were displayed. The red part represents normal tissue and the white part represents infarct tissue. **b** Quantitative analysis of infarct volume was analyzed. *$p < 0.05$ versus the sham-operated group, n = 5

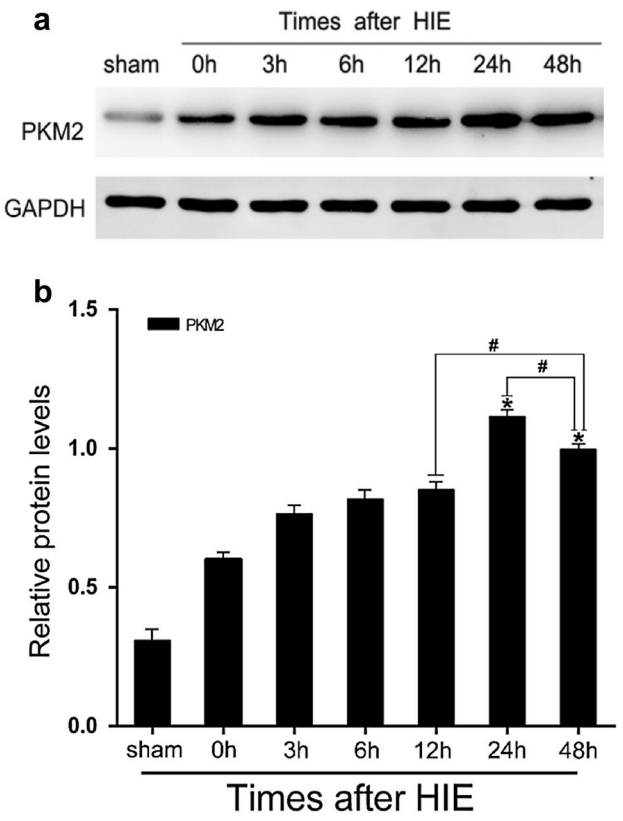

Fig. 2 PKM2 expression in newborn rat cerebral cortex in the ipsilateral hemisphere after HIE. **a** PKM2 expression in the brain cortex was detected by western blot in the HIE group compared to the sham group. The expression of PKM2 was gradually upregulated after HIE, peaked at 24 h and declined thereafter. **b** The bar chart shows the ratio of PKM2–GAPDH at different time points. *,#p < 0.05, n = 5

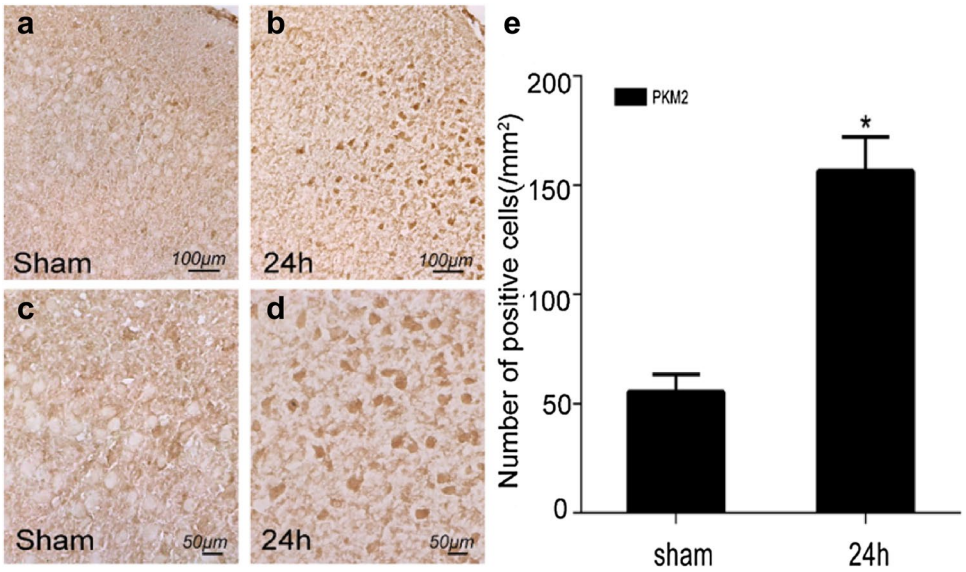

Fig. 3 The detection of PKM2 in the ipsilateral cerebral cortex with immunohistochemistry staining. **a, c** Sections were immunostained with antibody for PKM2 in the sham group and at 24 h after HIE (**b, d**). **e** Quantitative analysis of PKM2 positive cells in ipsilateral cerebral cortex. The number of PKM2 positive cells was increased in the cerebral cortex in 24 h time point HIE group compared with the sham group. *$p < 0.05$, n = 5

PKM2 was Localized in the Ipsilateral Cerebral Cortex Neurons After HIE

We conducted immunofluorescence to further investigate which cell type was the localization of PKM2 in the modeling HIE. The double-labeling immunofluorescence experiment was used to co-localize PKM2 with dissimilar cell-specific markers for neurons (NeuN), astrocytes (GFAP), microglia (IBa1).

Following HIE, co-staining with NeuN and PKM2 demonstrated that PKM2 was merely present in neurons of the ischemic penumbra of cortex, and the ratio of PKM2 positive neurons and all PKM2 positive cells was nearly 100% (Fig. 4c–e). However, PKM2 was barely expressed in astrocytes (Fig. 4f–h) or microglia (Fig. 4i–k) and the immunofluorescent staining of PKM2 and NeuN showed that the expression of PKM2 in the HIE group was markedly higher than that in the sham group (Fig. 4a–d). It demonstrated that the high expression of PKM2 in the HIE group was mainly in cortical neurons, signifying that PKM2 may be involved in the physiological changes of cortical neurons in neonatal rats after HIE.

PKM2 was Associated with Neuronal Apoptosis in the HIE Model

Neuronal apoptosis is deemed to be one of the most vital events after HIE. It is observed that changes in PKM2 expression mostly occurred in neurons. Therefore, it is reasonable to investigate whether PKM2 is related to neuronal apoptosis after neonatal HIE.

From our data, the expression of PKM2 in neurons was increased in the ipsilateral cerebral cortex after HIE, hence there was justification to speculate whether PKM2 is relevant in neuronal apoptosis. We quantified the expression of active caspase-3 after HIE using Western blot. From the Western Blot results, we can see that the expression level of active caspase-3 increased following HIE and maximized at the 24 h mark. This was consistent with the changes in PKM2 (Fig. 5a, b).

Additionally, to further explore the correlation between PKM2 and neuronal apoptosis, we carried out TUNEL staining to verify that PKM2 was associated with HIE-induced neuronal apoptosis. As shown in Fig. 5 (Fig. 5e–l), TUNEL-positive cells were co-labeled with PKM2 and neuron marker NeuN in the neonatal rat ipsilateral cortex at 24 h following HIE. This indicates that neuronal apoptosis had also occurred in the PKM2-expressing cells.

In recent years, researches have suggested that activated AKT could suppress cell apoptosis [27]. The p-AKT expression was shown to have down-regulated after HIE (Fig. 5c, d). An increased level of p-AKT following PKM2 knockdown in vitro indicated that PKM2 silencing was critical for AKT activation (Fig. 6c). Together, these results suggest that there is an association between PKM2 and neuronal apoptosis, which might be regulated by P-AKT signal pathway following HIE.

PKM2 Regulated Neuronal Apoptosis in Vitro

To further explore the specific role of PKM2 in neuronal apoptosis post HIE, we established OGD, an in vitro model which mimics the conditions of an in vivo HIE injury. We transfected the PKM2–siRNA into the rat primary cultures of cortical neurons (Fig. 6a, b). In accordance to the HIE model, the active caspase-3 protein level was decreased (Fig. 6c, d), while the p-AKT expression was specifically

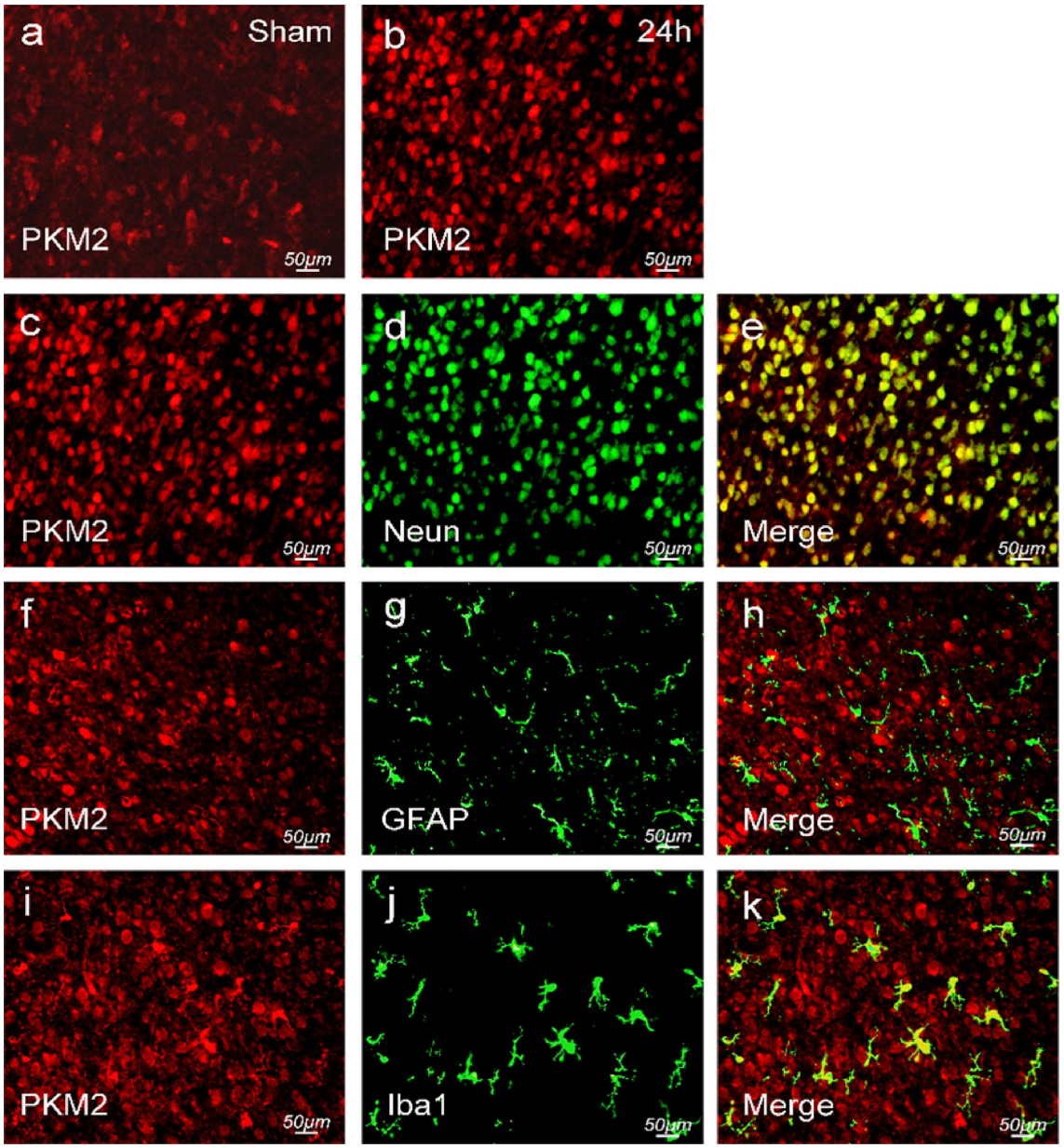

Fig. 4 PKM2 was localized in the ipsilateral cerebral cortex neurons after HIE. **a, b** Immunofluorescence showed that PKM2 expression increased at 24 h after HIE compared to the sham group. **c–e** Immunofluorescence staining showed that PKM2 was almost completely co-localized with neuron marker NeuN, not with astrocyte marker GFAP (**f–h**) or microglia marker Iba1 (**i–k**) in the ipsilateral cerebral cortex at 24 h after HIE. $^{*}p < 0.05$, n = 5

increased (Fig. 6e, f) after knocking down PKM2 and OGD treatment for 4 h and then reoxygenation for 24 h.

From MTT assay, si-PKM2#2 transfection prevented the decrease of neuron cell viability induced by OGD treatment (Fig. 6g). In addition, as immunofluorescent staining demonstrated that PKM2 silencing generated less co-labeling with PKM2 and active caspase-3 in the transfected cells, suggesting that neuronal apoptosis was reduced by knocking down PKM2 (Fig. 6h, i). When examined, these results suggest that PKM2 participated in neuronal apoptosis and the activation of p-AKT may depend on the corresponding mechanism.

Discussion

Using a clinically relevant model of neonatal hypoxia-ischemia, we investigated the role of PKM2 in neuronal apoptosis. As expected, TTC staining results for brain slices indicated evident variation in the HIE model

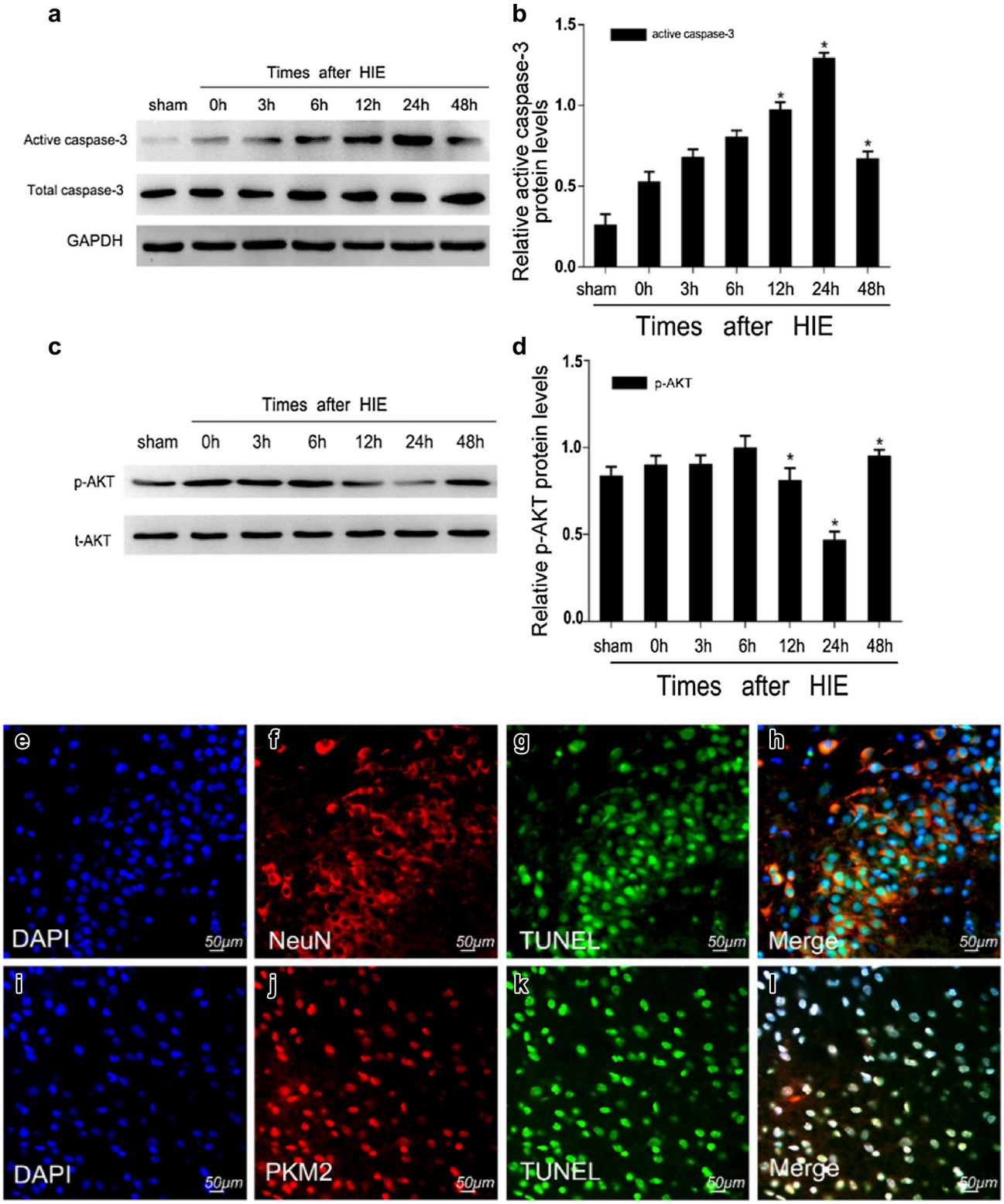

Fig. 5 Association of PKM2 with neuronal apoptosis in the ipsilateral cerebral cortex following HIE. **a** Active caspase-3 protein expression increased and peaked at 24 h following HIE. **b** Quantitative analysis (relative level) of expression of active caspase-3 at different time points. The bar chart shows the ratio of active caspase-3 to GAPDH at different time points. **c** p-AKT protein expression was decreased and bottom at 24 h. **e–h** TUNEL staining showed the colocalization of TUNEL-positive cells with PKM2 and neuron marker NeuN (**i–l**) in the rat ipsilateral cerebral cortex at 24 h following HIE. **d** The bar chart shows the ratio of p-AKT to t-AKT at different time points. $^{*}p < 0.05$, n = 5

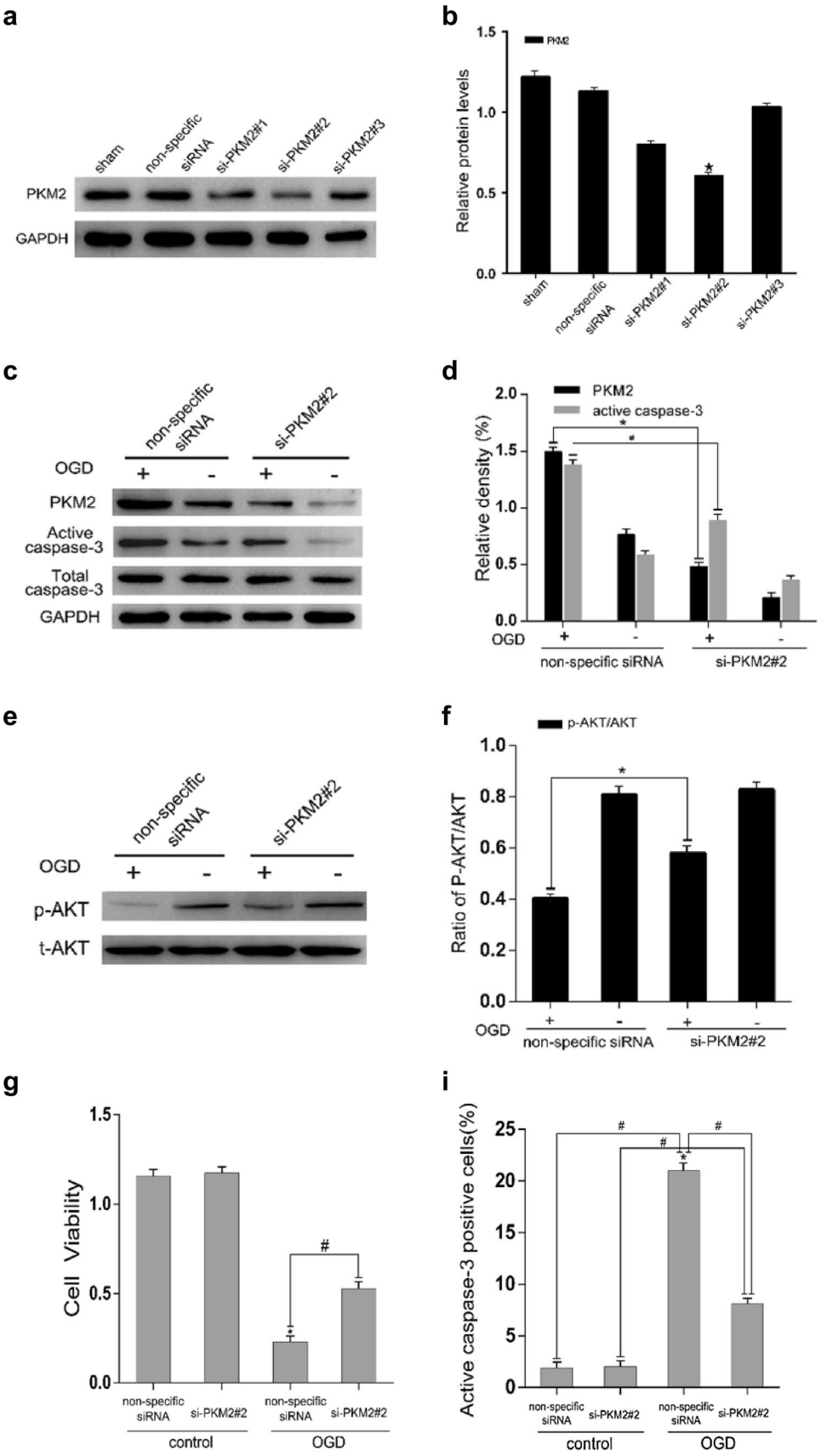

Fig. 6 Regulation of OGD-induced neuronal death by PKM2 expression. **a** PKM2–siRNAs were transfected into primary neurons to knock down PKM2 expression. **b** The bar chart shows the ratio of PKM2–GAPDH (*$p < 0.05$, $n = 3$). **c** PKM2 and active caspase-3 were downregulated in PKM2–siRNA group. **d** The bar chart indicates the density of PKM2 versus GAPDH (*,#$p < 0.05$, $n = 3$). **e** PKM2 silencing upregulated p-AKT protein expression levels. **f** The bar chart shows the density of p-AKT versus t-AKT (*$p < 0.05$, $n = 3$). **g** MTT assays were carried out to examine the effect PKM2 downregulation on OGD-induced alterations in neuronal metabolism (*$p < 0.05$, $n = 3$). **h** Immunofluorescent staining showed that colocalization between PKM2 and active caspase-3 in non-specific siRNA and PKM2–siRNA transfected primary neurons after OGD treatment. **i** The bar chart shows the number of active caspase-3 positive cells in the transfected cell (*$p < 0.05$, $n = 3$)

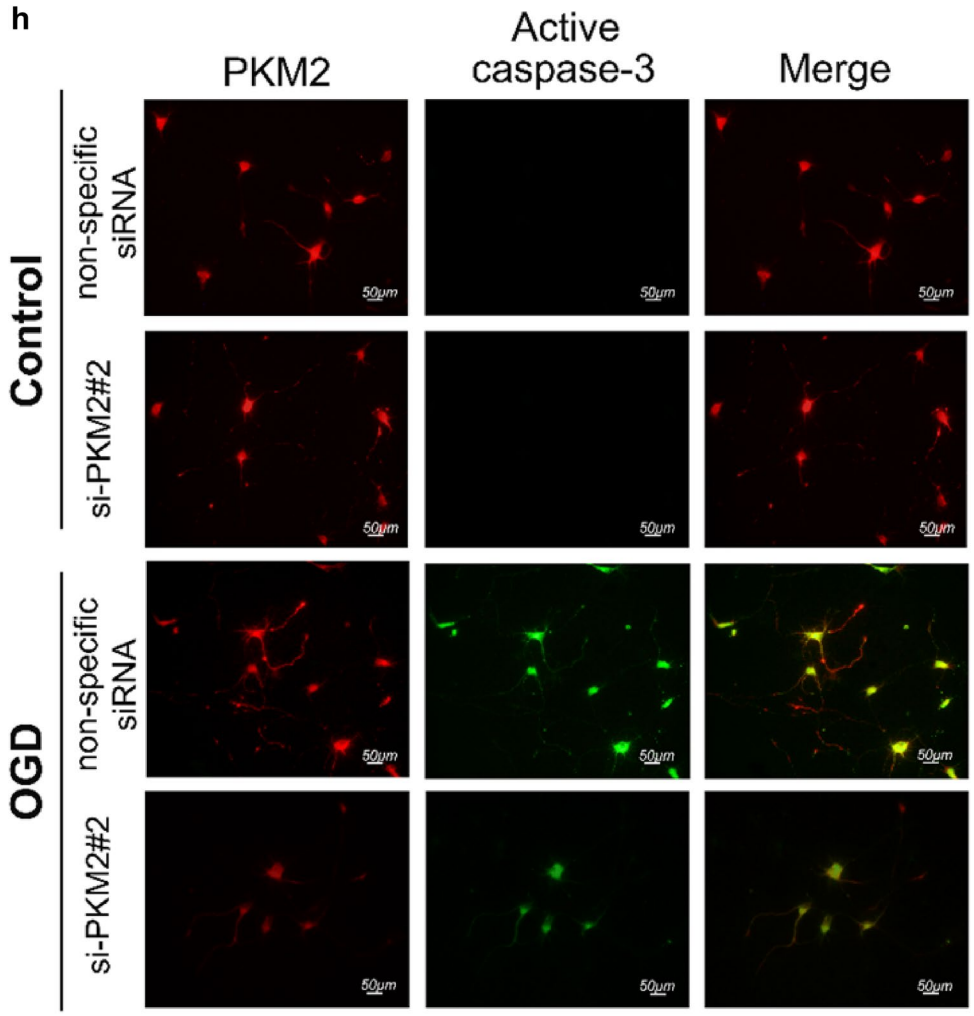

Fig. 6 (continued)

compared to the sham-operated group. The PKM2 expression was significantly up-regulated at 24 h after HIE in the cerebral cortex. Based on this data, we believe the increase in PKM2 and changes in other proteins measured by western blot were due to altered levels of expression within cells. In addition, immunohistochemistry analysis demonstrated the level of PKM2 expression in the cerebral cortex neurons after HIE was elevated dramatically compared to the sham-operated group. We found that PKM2 was mainly located in neurons of ipsilateral cerebral cortex, not in astrocytes or microglia. The increasing active caspase-3 expression and the decreasing p-AKT expression were parallel to PKM2 expression level in vivo. This result indicates that PKM2 may be involved in cortical neurons apoptosis after HIE. Meanwhile, we silenced PKM2 by siRNA in primary cultures of cortical neurons. This resulted in the reduction of active caspase-3 and the increase of p-AKT in the OGD in vitro model. Therefore, we came to the conclusion that PKM2 might promote neuronal apoptosis after HIE and that its activity may depend on the inactivation of p-AKT.

AKT activation results in activation of mTOR1 by phosphorylation and inhibition of TSC2; HIF1α expression is in turn induced by mTOR activation, and HIF1α enhances PKM2 expression through cooperating to c-Myc-hnRNPs splicing regulators [32]. Since AKT activation could inhibited cell apoptosis, the survival of PKM2 knockdown cells might require upregulation of p-AKT. In our vitro model, p-AKT expression was increased through transfecting PKM2–siRNA into primary cortical neuronal cells. Therefore, we assumed that PKM2 played a key role in the AKT-mediated signaling pathway by regulating the protein level of p-AKT and participated in the cortical neurons apoptosis. This finding corresponds to the phenomenon, showing that deprivation of PKM2 leads to activation of the AKT signaling pathway. The AKT signaling pathway activation in PKM2 knockdown cells was via the classical PI3K-Akt signaling pathway [27, 33, 34].

It is well known that PKM2 is universally expressed in embryogenesis, regeneration, and cancer [21, 35]. PKM2 also plays a significant role in cell division, tumor growth, angiogenesis, metastasis, and apoptosis [36]. However, in

recent studies using mouse models and RNASeq data sets analysis, PKM2 was also expressed in non-proliferating cells [17, 18, 37, 38]. In recent years, PKM2 and its role in relation to the regulation of cell proliferation had been explored and it is known that PKM2 plays a vital role in the transformation of many malignancies [36, 39]. The enhancive aerobic glycolysis and cell proliferation or migration originate in normal conditions and physiological growth and also occurs in cancer and therioma [40]. Our data differ from a previous report that showed PKM2 playing a role in up-regulating the expression of Bcl-xL protein, in the Bcl-2 family of proteins as an anti-apoptotic member, thereby inhibiting apoptosis and promoting tumor cell development [41]. We noticed that PKM2 has been confirmed as a biological marker for detection and diagnosis of tissue acute damage in the kidneys [42]. Presently, the role of PKM2 in response to HIE of newborn is unknown. However, unlike previous studies, we detected the expression of PKM2 on neuronal cells and explored its relationship with apoptosis. And this might be a potential therapeutic target and an important direction for our future research. The major strength of our study is the fact that it was the first time the relationship between PKM2 protein expression and apoptosis in non-proliferative cells, namely neonatal rat ipsilateral cortical neurons, was explored.

In conclusion, our study clearly indicates that PKM2 expression was increased significantly and these findings suggested a role for PKM2 in promoting apoptosis in newborn rat ipsilateral cortical neurons via AKT signaling pathway after HIE. These findings will make several contributions to investigating neuronal apoptosis in newborn rats following HIE. However, we would still need to conduct further research to explain the intrinsic molecular mechanisms regarding PKM2 and its role in regulating apoptosis events in cerebral cortex after HIE.

References

1. Charriaut-Marlangue C, Nguyen T, Bonnin P, Duy A, Leger P, Csaba Z, Pansiot J, Bourgeois T, Renolleau S, Baud O (2014) Sildenafil mediates blood-flow redistribution and neuroprotection after neonatal hypoxia-ischemia. Stroke 45:850–856
2. Threlkeld S, Lim Y, La Rue M, Gaudet C, Stonestreet B (2017) Immuno-modulator inter-alpha inhibitor proteins ameliorate complex auditory processing deficits in rats with neonatal hypoxic-ischemic brain injury. Brain Behav Immun 64:173–179
3. Lai M, Yang S (2011) Perinatal hypoxic-ischemic encephalopathy. J Biomed Biotechnol 2011:609813
4. Levene M, Kornberg J, Williams T (1985) The incidence and severity of post-asphyxial encephalopathy in full-term infants. Early Hum Dev 11:21–26
5. Cerio F, Lara-Celador I, Alvarez A, Hilario E (2013) Neuroprotective therapies after perinatal hypoxic-ischemic brain injury. Brain Sci 3:191–214
6. Huang B, Castillo M (2008) Hypoxic-ischemic brain injury: imaging findings from birth to adulthood. Radiographics 28:417–439. (**quiz 617**)
7. Martinez-Biarge M, Diez-Sebastian J, Kapellou O, Gindner D, Allsop J, Rutherford M, Cowan F (2011) Predicting motor outcome and death in term hypoxic-ischemic encephalopathy. Neurology 76:2055–2061
8. Douglas-Escobar M, Weiss M (2015) Hypoxic-ischemic encephalopathy: a review for the clinician. JAMA Pediatr 169:397–403
9. Lorek A, Takei Y, Cady E, Wyatt J, Penrice J, Edwards A, Peebles D, Wylezinska M, Owen-Reece H, Kirkbride V (1994) Delayed ("secondary") cerebral energy failure after acute hypoxia-ischemia in the newborn piglet: continuous 48-hour studies by phosphorus magnetic resonance spectroscopy. Pediatr Res 36:699–706
10. Vannucci R, Towfighi J, Vannucci S (2004) Secondary energy failure after cerebral hypoxia-ischemia in the immature rat. J Cereb Blood Flow Metab 24:1090–1097
11. Han B, DeMattos R, Dugan L, Kim-Han J, Brendza R, Fryer J, Kierson M, Cirrito J, Quick K, Harmony J, Aronow B, Holtzman D (2001) Clusterin contributes to caspase-3-independent brain injury following neonatal hypoxia-ischemia. Nat Med 7:338–343
12. Li Q, Li H, Roughton K, Wang X, Kroemer G, Blomgren K, Zhu C (2010) Lithium reduces apoptosis and autophagy after neonatal hypoxia-ischemia. Cell Death Dis 1:e56
13. Ma Q, Dasgupta C, Li Y, Bajwa N, Xiong F, Harding B, Hartman R, Zhang L (2016) Inhibition of microRNA-210 provides neuroprotection in hypoxic-ischemic brain injury in neonatal rats. Neurobiol Dis 89:202–212
14. Xu N, Zhang Y, Doycheva D, Ding Y, Zhang Y, Tang J, Guo H, Zhang J (2018) Adiponectin attenuates neuronal apoptosis induced by hypoxia-ischemia via the activation of AdipoR1/APPL1/LKB1/AMPK pathway in neonatal rats. Neuropharmacology 133:415–428
15. Tsutsumi H, Tani K, Fujii H, Miwa S (1988) Expression of L- and M-type pyruvate kinase in human tissues. Genomics 2:86–89
16. Williams A, Khadka V, Tang M, Avelar A, Schunke K, Menor M, Shohet R (2018) HIF1 mediates a switch in pyruvate kinase isoforms after myocardial infarction. Physiol Genom. https://doi.org/10.1152/physiolgenomics.00130.2017
17. Clower C, Chatterjee D, Wang Z, Cantley L, Vander Heiden M, Krainer A (2010) The alternative splicing repressors hnRNP A1/A2 and PTB influence pyruvate kinase isoform expression and cell metabolism. Proc Natl Acad Sci USA 107:1894–1899
18. Mazurek S (2011) Pyruvate kinase type M2: a key regulator of the metabolic budget system in tumor cells. Int J Biochem Cell Biol 43:969–980
19. Mazurek S, Boschek C, Hugo F, Eigenbrodt E (2005) Pyruvate kinase type M2 and its role in tumor growth and spreading. Semin Cancer Biol 15:300–308
20. Noguchi T, Yamada K, Inoue H, Matsuda T, Tanaka T (1987) The L- and R-type isozymes of rat pyruvate kinase are produced from a single gene by use of different promoters. J Biol Chem 262:14366–14371
21. Christofk H, Vander Heiden M, Harris M, Ramanathan A, Gerszten R, Wei R, Fleming M, Schreiber S, Cantley L (2008) The M2 splice isoform of pyruvate kinase is important for cancer metabolism and tumour growth. Nature 452:230–233
22. Lee J, Kim H, Han Y, Kim J (2008) Pyruvate kinase isozyme type M2 (PKM2) interacts and cooperates with Oct-4 in regulating transcription. Int J Biochem Cell Biol 40:1043–1054
23. Cairns R, Harris I, Mak T (2011) Regulation of cancer cell metabolism. Nat Rev Cancer 11:85–95
24. Tech K, Tikunov AP, Farooq H, Morrissy AS, Meidinger J, Fish T, Green SC, Liu H, Li Y, Mungall AJ, Moore RA (2017) Pyruvate kinase inhibits proliferation during postnatal cerebellar

neurogenesis and suppresses medulloblastoma formation. Cancer Res 77:3217–3230
25. Steták A, Veress R, Ovádi J, Csermely P, Kéri G, Ullrich A (2007) Nuclear translocation of the tumor marker pyruvate kinase M2 induces programmed cell death. Cancer Res 67:1602–1608
26. Dixon B, Reis C, Ho W, Tang J, Zhang J (2015) Neuroprotective strategies after neonatal hypoxic ischemic encephalopathy. Int J Mol Sci 16:22368–22401
27. Qin X, Du Y, Chen X, Li W, Zhang J, Yang J (2014) Activation of Akt protects cancer cells from growth inhibition induced by PKM2 knockdown. Cell Biosci 4:20
28. Cai J, Kang Z, Liu W, Luo X, Qiang S, Zhang J, Ohta S, Sun X, Xu W, Tao H, Li R (2008) Hydrogen therapy reduces apoptosis in neonatal hypoxia-ischemia rat model. Neurosci Lett 441:167–172
29. Ma D, Hossain M, Chow A, Arshad M, Battson R, Sanders R, Mehmet H, Edwards A, Franks N, Maze M (2005) Xenon and hypothermia combine to provide neuroprotection from neonatal asphyxia. Ann Neurol 58:182–193
30. Rice JE, Vannucci RC, Brierley JB (1981) The influence of immaturity on hypoxic-ischemic brain damage in the rat. Ann Neurol 9:131–141
31. Li B, Concepcion K, Meng X, Zhang L (2017) Brain-immune interactions in perinatal hypoxic-ischemic brain injury. Prog Neurobiol 159:50–68
32. Sun Q, Chen X, Ma J, Peng H, Wang F, Zha X, Wang Y, Jing Y, Yang H, Chen R, Chang L, Zhang Y, Goto J, Onda H, Chen T, Wang M, Lu Y, You H, Kwiatkowski D, Zhang H (2011) Mammalian target of rapamycin up-regulation of pyruvate kinase isoenzyme type M2 is critical for aerobic glycolysis and tumor growth. Proc Natl Acad Sci USA 108:4129–4134
33. Kanda R, Kawahara A, Watari K, Murakami Y, Sonoda K, Maeda M, Fujita H, Kage M, Uramoto H, Costa C, Kuwano M, Ono M (2013) Erlotinib resistance in lung cancer cells mediated by integrin β1/Src/Akt-driven bypass signaling. Cancer Res 73:6243–6253
34. Wang C, Jiang J, Ji J, Cai Q, Chen X, Yu Y, Zhu Z, Zhang J (2017) PKM2 promotes cell migration and inhibits autophagy by mediating PI3K/AKT activation and contributes to the malignant development of gastric cancer. Sci Rep 7:2886
35. Garnett M, Dyson R, Dost F (1974) Pyruvate kinase isozyme changes in parenchymal cells of regenerating rat liver. J Biol Chem 249:5222–5226
36. He X, Du S, Lei T, Li X, Liu Y, Wang H, Tong R, Wang Y (2017) PKM2 in carcinogenesis and oncotherapy. Oncotarget 8:110656–110670
37. Dayton T, Gocheva V, Miller K, Israelsen W, Bhutkar A, Clish C, Davidson S, Luengo A, Bronson R, Jacks T, Vander Heiden M (2016) Germline loss of PKM2 promotes metabolic distress and hepatocellular carcinoma. Genes Dev 30:1020–1033
38. David C, Manley J (2010) Alternative pre-mRNA splicing regulation in cancer: pathways and programs unhinged. Genes Dev 24:2343–2364
39. Gao X, Wang H, Yang JJ, Liu X, Liu ZR (2012) Pyruvate kinase M2 regulates gene transcription by acting as a protein kinase. Mol cell 45:598–609
40. Lunt SY, Vander Heiden MG (2011) Aerobic glycolysis: meeting the metabolic requirements of cell proliferation. Annu Rev Cell Dev Biol 27:441–464
41. Kwon O, Kang T, Kim J, Kim M, Noh S, Song K, Yoo H, Kim W, Xie Z, Pocalyko D, Kim S, Kim Y (2012) Pyruvate kinase M2 promotes the growth of gastric cancer cells via regulation of Bcl-xL expression at transcriptional level. Biochem Biophys Res Commun 423:38–44
42. Cheon JH, Kim SY, Son JY, Kang YR, An JH, Kwon JH, Song HS, Moon A, Lee BM, Kim HS (2016) Pyruvate kinase M2: a novel biomarker for the early detection of acute Kidney injury. Toxicol Res 32:47–56